1.D.1 *Nuclear Physics* **A138** (1969) 273—304; © *North-Holland Publishing Co., Amsterdam*


# THE STRUCTURE OF THE sd SHELL NUCLEI (IV). $^{20}$Ne, $^{21}$Ne, $^{22}$Ne, $^{22}$Na AND $^{24}$Mg

Y. AKIYAMA †
*Department of Physics,*
*University of Michigan, Ann Arbor, Michigan*
A. ARIMA ††
*Department of Physics,*
*Rutgers, The State University, New Brunswick, New Jersey*
and
T. SEBE †††
*Chalk River Nuclear Laboratories,*
*Chalk River, Ontario, Canada*

Received 3 July 1969

**Abstract:** The shell model with the phenomenological effective interaction is applied to study level structures of $^{20}$Ne, $^{21}$Ne, $^{22}$Ne, $^{22}$Na and $^{24}$Mg. The full basis in the sd shell is taken in $^{20}$Ne to diagonalize the energy matrices. This example confirms that $SU_3$ symmetry and the supermultiplet provide a very good way of truncation. This truncation is used to calculate level schemes of many nuclei beyond $^{20}$Ne. Even though deviations of the effective interaction from the pure Q-Q interaction and the spin-orbit interaction break the $SU_3$ symmetry and the supermultiplet, the main components of calculated wave functions in low-lying energies can be very well labelled by these two symmetries. Generally, good agreement with observations is found. Particularly, the lowest rotational bands are nicely explained. Exceptions are the level structure of $^{22}$Na and $\frac{1}{2}^+$ in $^{19}$O and $^{21}$Ne, which are too low in the calculation, and the $K = 2$ bands in $^{22}$Ne and $^{24}$Mg, which are again too low in the calculation.

## 1. Introduction

Extensive data have been recently accumulated on the sd shell nuclei. These nuclei are very interesting from a theoretical point of view, because they are very appropriate for a study of the applicability of nuclear models, the property of the residual interactions and the mechanism of nuclear rotational motion.

Among a number of models, the nuclear shell model is one of the most successful, where residual forces play a very important role [1–5]). These interactions can induce configuration mixings, which can sometimes be interpreted as rotational motion. A study of nuclei in the sd shell can thus lead to a better understanding between a microscopic description of the nucleus (shell model) and a macroscopic (collective) description [7]).

† On leave of absence from College of General Education, University of Tokyo, Tokyo.
†† Present address: Department of Physics, University of Tokyo, Tokyo.
††† Present address: Department of Applied Physics, Hosei University, Koganei, Tokyo.

The structure of $^{20}$Ne is studied again in this paper to reconfirm that the symmetric group (the supermultiplet) [6]) and the $SU_3$ group provide a very good way of truncation [2]). Employing the truncation above described we calculate the level structures of $^{21}$Ne, $^{21}$F, $^{22}$Ne, $^{22}$Na and $^{24}$Mg.

The low-energy spectra of the nuclei studied have rotational features, which are very nicely explained by our calculation. We find that the moment of inertia is not sensitive to the nature of the residual forces, which means that the rotational motion has a very simple structure and is rather independent of the detailed property of interactions, for example, the radial dependence of interactions. On the other hand, the positions of the heads in the gamma and beta bands are varied very much when a residual interaction is changed, for example from the Yukawa to the Gaussian. The positions of these excited bands, therefore, give very crucial restrictions on the residual interactions. This situation was already found in the previous $\chi^2$ fit calculation of the isotopes of O, F and Ne [ref. [5])].

Our calculations predict the gamma bands in even nuclei and the excited band in the odd nuclei at too low energies. It is particularly interesting to find quite similar results between our restricted calculation and the more extensive calculation recently [8]) performed in the Oak Ridge National Laboratory up to $^{22}$Na. In the Oak Ridge calculation, all the states in a full shell-model calculation were considered, and very good agreement with the experimental spectrum could be found except for the excited bands, which were too low in energy. A direct comparison between these two calculations is not possible because our simple residual interactions are unfortunately different from theirs. (In the Oak Ridge calculation, the Kuo-Brown and Kuo forces [9]) were used.) In order to predict the excited bands in the correct positions, we would either have to modify both kinds of interactions or consider the larger set of basis states. We have noted that the results from our calculation give better agreement with those from Oak Ridge if the s-orbit in our calculation is pushed up by about 1 MeV in $^{21}$Ne and $^{22}$Ne. This means that their effective interactions can produce automatically this shift of the s-orbit, which is an advantage of their potentials, although this shift is not large enough to attain agreement with experiment. The shift of the s-orbit affects particularly the energy of the lowest $\frac{1}{2}^+$ level in $^{21}$Ne. Therefore, it would be important for us to find a better effective interaction which can push up this s-orbit relatively to the d-orbit in the middle of the shell.

The electromagnetic transitions are calculated in $^{20}$Ne, but those in other nuclei and the spectroscopic factors will be discussed in a forthcoming paper.

## 2. The model

According to the shell model, we assume that the $^{16}$O nucleus constitutes a tightly bound system, which is treated as the core in our calculation. In the nuclei having a few extra nucleons outside of $^{16}$O, the energies of the low-lying levels can be well described by the degree of freedom of the particles in the outmost shell, except for

certain levels which are suggested to be the core excited states. The single-particle energy levels can be deduced from the observed level structures of $^{17}$O and $^{17}$F. We take only the single-particle levels with positive parity, which restricts our calculations to positive-parity states.

Our model Hamiltonian is assumed to have the form

$$H = H_0 + H_S + V,$$

where $H_0$ is the Hamiltonian of the core and

$$H_S = \sum_{i \text{ (outside the core)}} \left\{ -\frac{\hbar^2}{2m}\nabla_i^2 + \tfrac{1}{2}(m\omega^2) r_i^2 + \tfrac{1}{6}\varepsilon(l_i^2 - 6) + \xi(l_i S_i) \right\}, \tag{1}$$

and $V = \sum_{i<j} V_{ij}$, which will be called the residual interaction. The field produced by the core is replaced by the harmonic oscillator well, the spin-orbit interaction and the modification of the single-particle energy of the $s_{\frac{1}{2}}$ orbit. It is apparently certain that the single-particle potential, which has the correct asymptotic behavior outside the nuclear radius, is a better approximation than the harmonic oscillator potential, but a modification induced by the more realistic potential has never been shown to be important except in one case, which has already been discussed by us concerning the excited $0^+$ in $^{18}$O. It is still, however, an important problem to use a more realistic single-particle potential [10]) to see what effect it can have in many-body calculations. Using the observed level structures of $^{17}$O, we can obtain

$$\xi = 2.03 \text{ MeV}, \quad \varepsilon = 1.15 \text{ MeV}. \tag{2}$$

A slightly different set of $\xi$ and $\varepsilon$ can be found in $^{17}$F. We fix $\xi$ to be 2 MeV but change $\varepsilon$ a little sometimes, because $\varepsilon$ induces fairly large modifications in the calculated levels. Smaller $\varepsilon$ (about 0 MeV) seems to give better agreement with the observations beyond $^{20}$Ne. This is also pointed out by Bouten, Elliott and Pullen [11]).

It is assumed that the residual interactions $V_{ij}$ between pairs of nucleons outside the $^{16}$O core are central and of the form

$$V_{12} = -({}^{13}VP_{13} + {}^{31}VP_{31} + {}^{11}VP_{11} + {}^{33}VP_{33}) f(r_{13}), \tag{3}$$

where $P_{2T+1,2S+1}$ is the projection operator to the state of isospin $T$ and spin $S$ in which the strength of the residual interaction is expressed by ${}^{2T+1,2S+1}V$. The Yukawa $e^{-r/r_0}/(r/r_0)$ and the Gaussian $e^{-(r/r_0)^2}$ radial dependences are employed as $f(r)$.

The radial parts of the oscillator functions are assumed for the single-particle wave functions

$$R_{0d}(r) = \frac{4\nu^{\frac{7}{4}}}{15^{\frac{1}{2}}\pi^{\frac{1}{4}}} r^2 e^{-\frac{1}{2}\nu r^2},$$

$$R_{1s}(r) = \frac{2^{\frac{1}{2}}\nu^{\frac{3}{4}}}{3^{\frac{1}{2}}\pi^{\frac{1}{4}}} (3 - 2\nu r^2) e^{-\frac{1}{2}\nu r^2}. \tag{4}$$

The Slater integrals depend on a parameter

$$\lambda = r_0\sqrt{\tfrac{1}{2}\nu}. \tag{5}$$

We fix rather arbitrarily this $\lambda$ to be $\frac{2}{3}$ for the Yukawa and 0.7 for the Gaussian interaction. The Coulomb energy difference between $^{17}$O and $^{17}$F enables us to estimate $\nu$ to be 0.362 fm$^{-2}$. Our assumed values of $\lambda$ correspond to $r_0 = 1.58$ fm for the Yukawa and $r_0 = 1.66$ fm for the Gaussian interaction respectively. The magnitudes of $^{13}V$, $^{31}V$, $^{11}V$ and $^{33}V$ are given the following values for the Yukawa interaction:

$$^{13}V = 35.0 \text{ MeV}, \ ^{31}V = 27.0 \text{ MeV}, \ ^{11}V = 0.0 \text{ MeV}, \ ^{33}V = -13.5 \text{ MeV}, \tag{6}$$

because they give the best agreement with the experiments on $^{18}$O and $^{18}$F. Somewhat different values for $V$ are chosen in some nuclei to provide better agreement with observations. The values for the Gaussian interaction are:

$$^{13}V = 60.0 \text{ MeV}, \ ^{31}V = 45.0 \text{ MeV}, \ ^{11}V = 0.0 \text{ MeV}, \ ^{21}V = -22.5 \text{ MeV}. \tag{7}$$

The relative ratios between these magnitudes of $^{2T+1,2S+1}V$ for the Gaussian interaction are kept approximately the same as those in the Yukawa interaction. Slightly weaker potentials than those with parameters mentioned above give better agreement below $^{20}$Ne, while slightly stronger ones give better results beyond $^{20}$Ne.

The two-body interaction has definitely non-central parts. It would therefore be desirable to introduce such parts and further to use a more realistic central potential than the interactions adopted above. These problems will be discussed in the future, although our phenomenological analysis of two- and three-body system seems to show that non-central interactions are unimportant [3]).

We must briefly describe how to construct the many-body wave functions. One of the authors (Akiyama) has calculated the Clebsch-Gordan coefficients and the coefficients of fractional parentages of the $SU_3$ and $SU_6$ classification schemes. These coefficients have been partially published already and others will be published elsewhere [12]). These coefficients are extremely useful in calculating matrix elements of one- and two-body operators. The Racah coefficients of the $SU_3$ group, which have been algebraically expressed by Hecht [13]), are useful to construct the coefficients of fractional parentage of two-particle coupling.

### 3. Brief review of two- and three-body systems

Figs. 1 and 2 show the level structures of $^{18}$O and $^{18}$F. In our calculations using the Yukawa interaction the levels of $^{18}$O are well reproduced except for the excited $0^+$ state. One possible way to push up this level was shown in our previous paper with a modification of the 1s wave function [2]). In fig. 1, $y$ measures this modification with $y$ defined in ref. [2]). This possibility is now being studied completely by Nachamkin and Harvey in Chalk River with the Woods-Saxon potential [10]).

The Gaussian interaction gives higher and better energy to this $0^+$ state in $^{18}O$. The position of the excited $0^+$ state is very sensitive to the nature of the potential. The $0^+$ in $^{18}O$ state is an example, and other examples can be seen in $^{20}Ne$. The effective interactions derived by Kuo and Brown give very nice agreement with the observation [9]). There is an observed strong E2 decay from this $0^+$ state to the first $2^+$ state. This decay probability is too strong to be explained by the simple shell

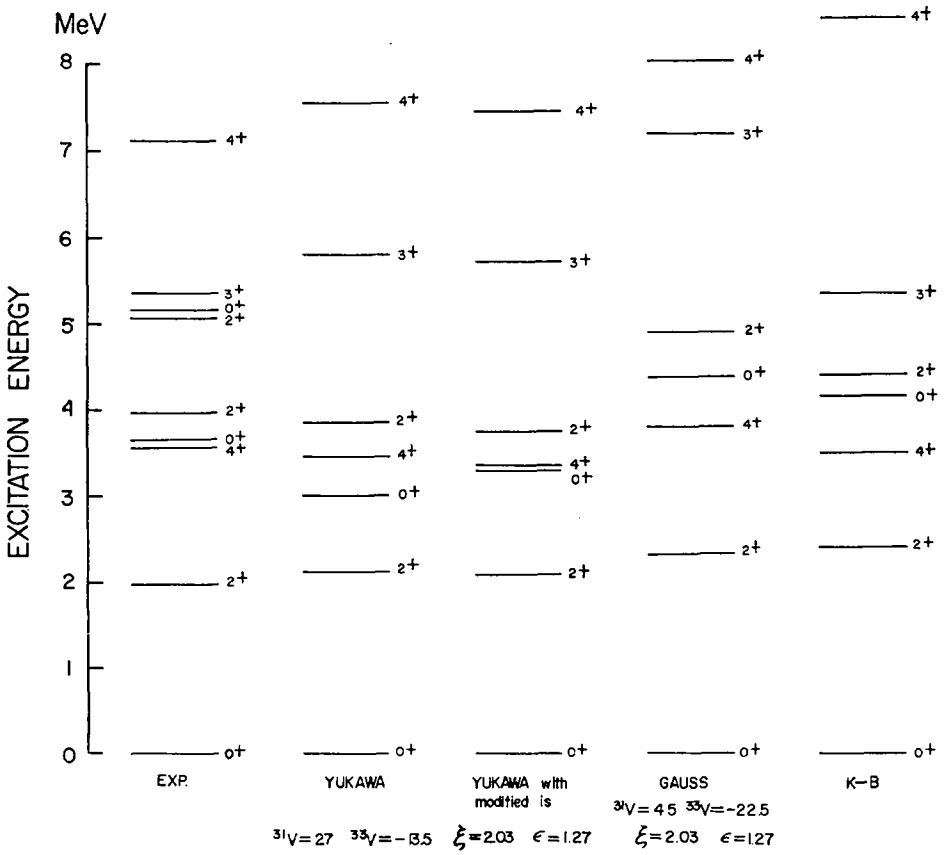


Fig. 1. Energy levels of $^{18}O$[31]). K-B shows the result obtained by use of effective interactions derived by Kuo and Brown. Exp. shows the observed level scheme.

model [2]), which requires the admixture of the core excited states [14,15]). In order to explain this E2 transition, a 25–30 % admixture of the core-excited state in both the 3.63 MeV $0^+$ and the 1.98 MeV $2^+$ levels of $^{18}O$ is required [5]). The position of the $0_2^+$ level can be greatly affected by the admixture, but it has not yet been determined which effect among the modification of the 1s wave, the admixture of the core-excited state or the modification of the potential is most responsible for the location of the $0_2^+$ level.

The low-lying states below 1.13 MeV are nicely explained by our calculation in $^{18}$F. Both our calculations and those of Kuo and Brown have, however, failed to predict the $1^+$ level at 1.7 MeV. This level has been suggested to be the 4p–2h [refs. [3,16,17])]. Such experiments as $^{14}$N (Li, d)$^{18}$F are highly desirable in order to check this conjecture [36]). A $2^+$ level has been observed at 2.53 MeV. Our central force produces a $2^+$ level slightly higher in energy than the observed 2.53 MeV, but it was shown in our previous paper that an addition of a weak attractive tensor force to the effective interaction (3) can bring this level down to the correct energy [3]). This level therefore has the possibility of belonging to the $(sd)^2$ configuration[3]). Two

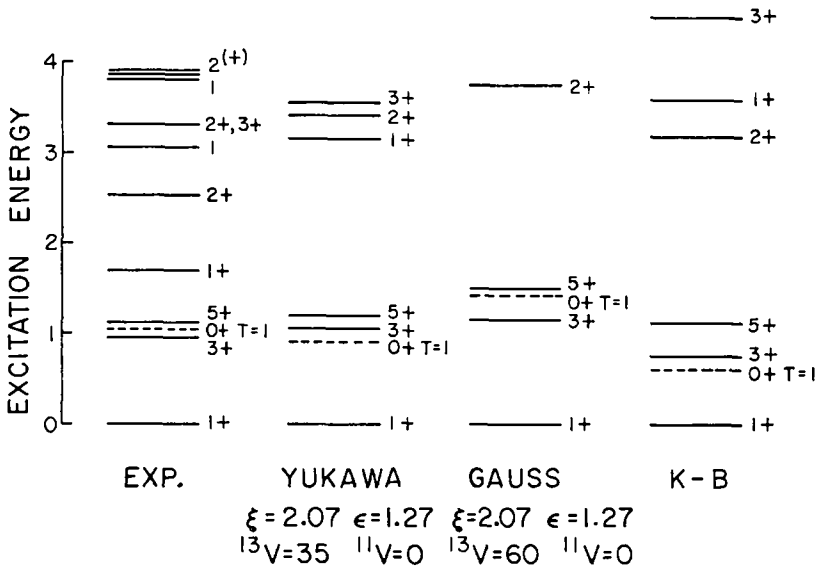


Fig. 2. Energy levels of $^{18}$F [ref. [31])].

other levels at 2.1 MeV and 1.09 MeV have presumably negative parity or are core-excited states, since no corresponding states can be found in our calculation.

The calculated spectrum for the nucleus $^{19}$O has the poorest agreement with experiment (see fig. 3(a)). All of the local central potentials fail to give the correct level structure of this nucleus. The effective interactions of Kuo and Brown produce a slightly better result, but still the $\frac{1}{2}^+$ state is too low in energy [8]). Thus, the level structure of $^{19}$O is not yet clearly understood. This nucleus has only three nucleons but is sufficiently complicated to provide good information about the nature of effective interactions.

Although the nucleus $^{19}$O is the worst case, the other three-nucleon nucleus, $^{19}$F, is described remarkably well by the shell model (see fig. 3(b)). There is a rotational $K = \frac{1}{2}$ band based on the ground state, which is very nicely reproduced by any set of

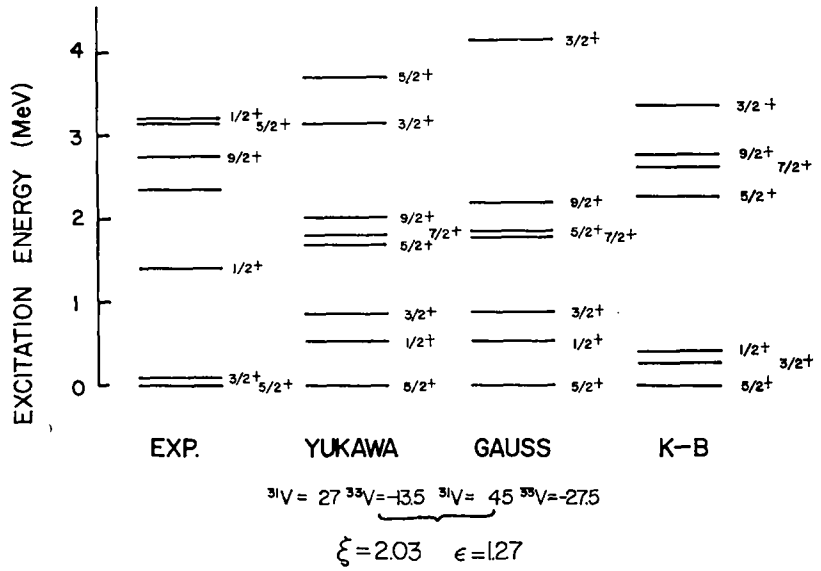


Fig. 3(a). Energy levels of $^{19}O$ [ref. $^{31}$)].

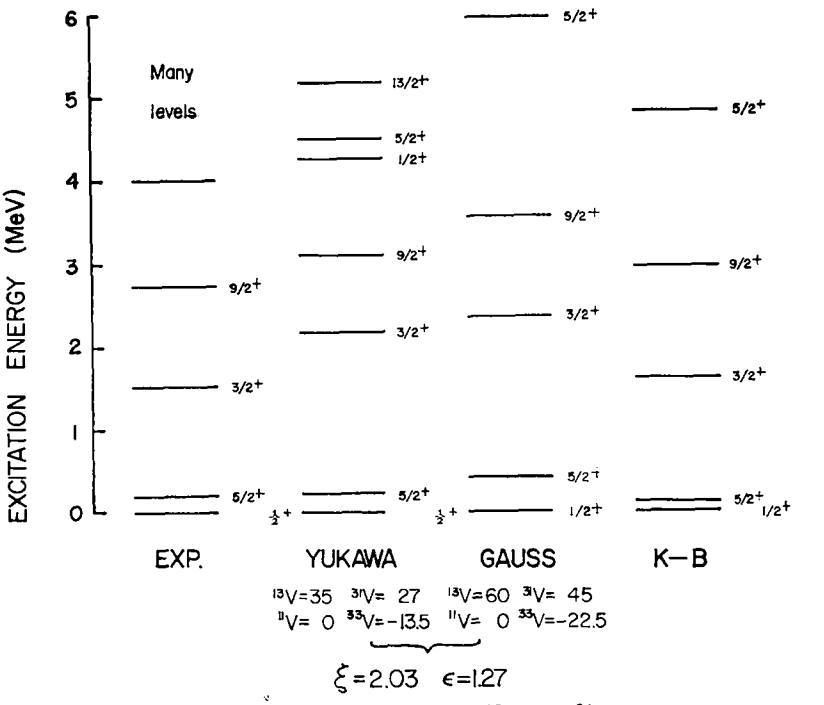


Fig. 3(b). Energy levels of $^{19}F$ [ref. $^{31}$)].

interactions. Two rotational bands are theoretically expected to start around 4 MeV. It was suggested that these two bands have negative deformation [18]), (oblate shape),

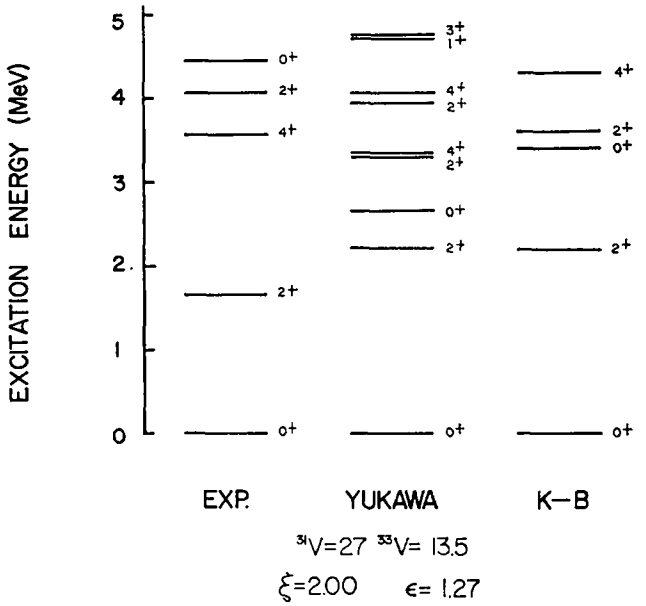


Fig. 4(a). Energy levels of $^{20}O$ [ref. [31])].

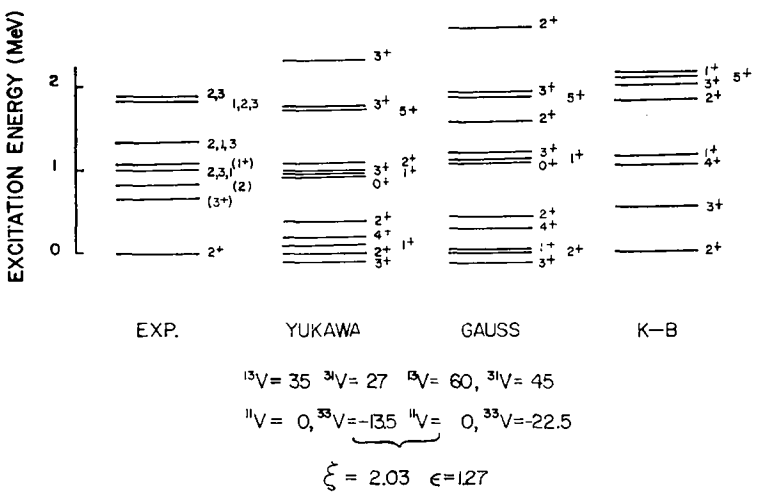


Fig. 4(b). Energy levels of $^{20}F$ [ref. [31])].

while the ground state band has the prolate shape. It will be very interesting to find the $\frac{1}{2}^-_1$ and $\frac{1}{2}^-_3$ levels belonging to the ground band and to determine the shapes of the bands which start around 4 MeV.

The level structures of $^{20}$O and $^{20}$F are shown in figs. 4(a) and (b). The phenomenological potential gives very poor agreement in $^{20}$F, where [31] $T = S = 1$ states are dominant, and therefore non-central forces can play an important role and modify the prediction. In these nuclei, the leading $SU_3$ states, e.g. (42) in $^{20}$O and (61) in $^{20}$F, carry only 50 % and 65 % probabilities. This is reasonable because these nuclei are expected to be spherical.

## 4. The level structure of $^{20}$Ne

### 4.1. ROTATIONAL LEVEL AND KINKING

The structure of $^{20}$Ne was thoroughly studied in our first paper [2]), in which we found that the symmetry and the $SU_3$ group provide a very good way of truncation. Fig. 5(a) shows the calculated and observed level schemes. The parameter $\varepsilon$, which gives the energy difference between the s-orbit and the d-orbit, greatly affects the rotational structure; a smaller $\varepsilon$ gives a larger deviation from the rotational structure. Furthermore the position of the first excited $0^+$ state is sensitive to this $\varepsilon$. In order to obtain good agreement with the observed ground $K = 0$ band, $\varepsilon$ should be about 1 MeV when the Yukawa shape is used. In fact, the levels of the ground rotational band are reproduced both in the Yukawa and Gaussian interactions. In particular, if we use a somewhat stronger Yukawa interaction ($^{13}V = 36.75$, $^{31}V = 28.50$, $^{11}V = 0.0$ and $^{33}V = 14.25$) and a slightly weaker Gaussian interaction ($^{13}V = 55$, $^{31}V = 42.43$, $^{11}V = 0$ and $^{33}V = 21.21$), the agreement with experiments is surprisingly good as far as the ground rotational band is concerned.

Kuehner and Pearson have pointed out that the energies of the ground state band deviate from the general form expected from a rotational band [19])

$$E_0 = A + BJ(J+1) + cJ^2(J+1)^2.$$

The excitation energies exhibit kinks when plotted as a function of $J(J+1)$ as in fig. 5(b). The energies for the pure $SU_3$ states of (80) can deviate from a straight line (fig. 5b) but cannot give the kinking phenomenon; thus one suspects that this kinking is induced by other $(\lambda\mu)$ states which the deviation of the residual interaction from the pure quadrupole force admixes. Indeed, it has been shown by Kalman *et al.* that the Q-Q + pairing-interaction model will give a spectrum with kinks [20]). The spectrum arising from our effective interactions also has kinks (fig. 5b). In our case the residual interaction modifies the results given by the simple $SU_3$ model by pushing down the $0^+$, $4^+$ and $8^+$ states more than the $2^+$ and $6^+$ states from the energies for the pure $SU_3$ states of (80). This seems to explain the "kinking". It is further interesting to find a certain correlation between this kinking and the percentages of the (80) components in wave functions. This correlation is shown in table 1; the $0^+$, $4^+$ and $8^+$ states are more contaminated by other $(\lambda\,\mu)$ states than the $2^+$ and $6^+$ states. These contaminations into the (80) main components are induced by two mechanisms. One of them is the deviation of the residual central force from

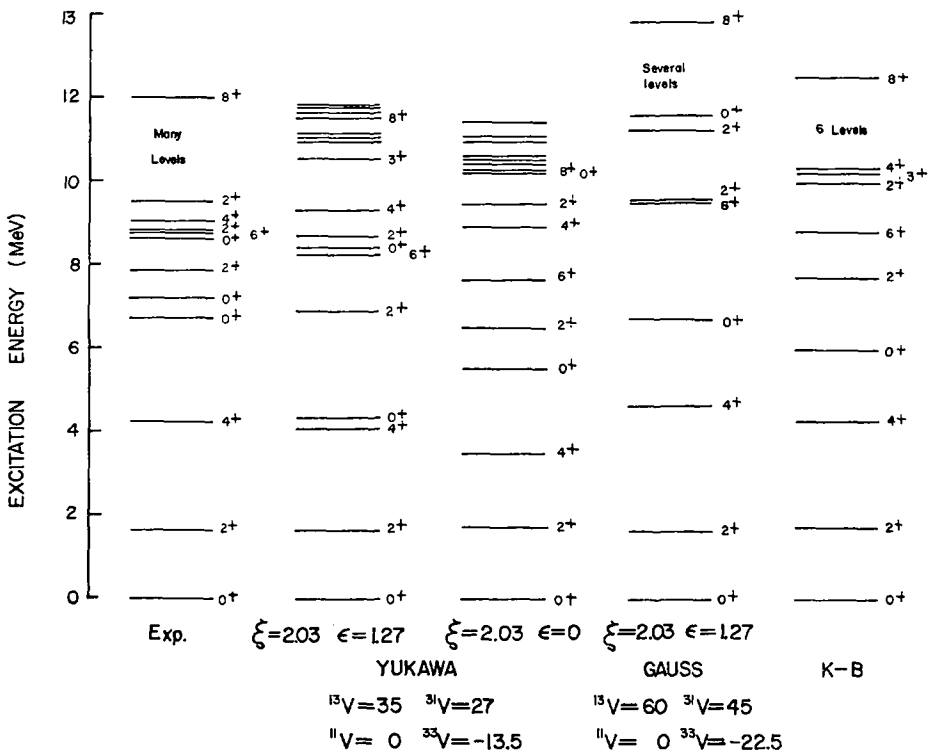


Fig. 5(a). Energy levels of $^{20}$Ne [ref. $^{31}$)].

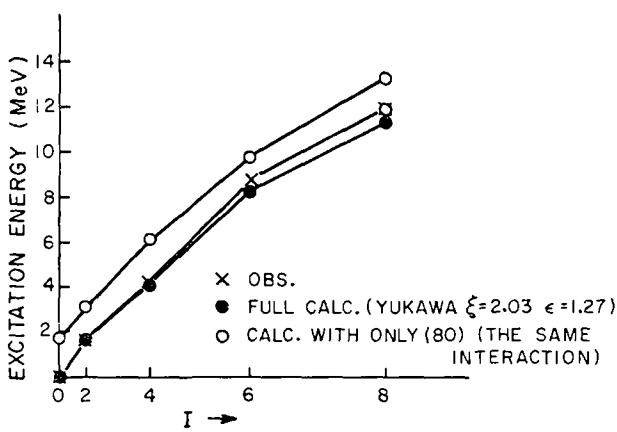


Fig. 5(b). Rotational levels of $^{20}$Ne. The excited-state energies are plotted as a function of $I(I+1)$. In this figure $I$ is indicated instead of $I(I+1)$ in the abscissa.

the simple Q-Q interaction, which induces the admixtures of the (42) and (04) components in the [4] symmetry (i.e. the mechanism suggested by Kalman *et al.*). The other is the spin-orbit interaction, which mixes mainly the (61) of the [31] symmetry.

TABLE 1

Squared amplitudes of the (80) component in the wave functions of the ground rotational band in $^{20}$Ne

| $J$ | Squared amplitude of (80) |
|---|---|
| $0^+$ | 0.895 |
| $2^+$ | 0.906 |
| $4^+$ | 0.848 |
| $6^+$ | 0.875 |
| $8^+$ | 0.806 |

$\xi = 2.0\ \varepsilon = 1.2$ and Gaussian; $^{13}V = 60$, $^{31}V = 45$, $^{11}V = 0$, $^{33}V = -22.5$.

### 4.2. THE EXCITED $K = 0$ BAND

The Yukawa interaction with the reasonable value of $\varepsilon = 1.27$ which gives better agreement to the lowest band, predicts the excited $0^+$ state at too low an energy, while the Gaussian interaction gives the correct energy to this excited state. This level provides consequently a very important condition to determine the nature of the residual interaction, which can explain very well why this level played a very important role in the $\chi^2$ fitting procedure [5]). The observed level scheme has at least two $0^+$ levels around 7 MeV excitation. Our present calculation only predicts one $0^+$ level. Also the $\chi^2$ fitting calculation [5]) cannot predict more than one $0^+$ state around 7 MeV, though the possibility that a configuration having $d_{\frac{3}{2}}$ particles is found in low energy cannot be eliminated because the $d_{\frac{3}{2}}$ orbit is not taken into account in this $\chi^2$ fitting procedure. Both our present calculation and the $\chi^2$ fitting calculation suggest consistently the possibility of a core-excited state.

There are two $2^+$ states just above the two $0^+$ states at 7.46 MeV and 7.90 MeV. Our calculation predicts only one $2^+$ level. The calculation performed in the Oak Ridge National Laboratory shows a very similar result, although there the two-body matrices given by Kuo and Brown were used. It would be very interesting to measure the $B$(E2) between these $2^+$ states and $0^+$ states to decide which states comprise a rotational family.

### 4.3. ELECTROMAGNETIC TRANSITIONS

The $B$(E2) values are calculated in several cases (table 2), among them the transitions $2_1^+ \rightarrow 0_1^+$, $4_1^+ \rightarrow 2_1^+$, $6_1^+ \rightarrow 4_1^+$ and $0_2^+ \rightarrow 2_1^+$ are observed. If 0.583 $e$ is taken as an effective charge, i.e. $e_p = 1.583\ e$ and $e_n = 0.583\ e$, the $B(\mathrm{E2}\ 2_1^+ \rightarrow 0_1^+)$ is very nicely reproduced. The $B$(E2) values do not, however, deviate so much from those given by the $SU_3$ model, except $B(\mathrm{E2}\ 0_2^+ \rightarrow 2_1^+)$. Therefore, we have a very enhanced

$B(\mathrm{E2}\ 4_1^+ \rightarrow 2_1^+)$ between the second and the first excited states, which is larger by 30 % than $B(\mathrm{E2}\ 2_1^+ \rightarrow 0_1^+)$. According to the observation, the situation is quite different, and $B(\mathrm{E2}\ 4_1^+ \rightarrow 2_1^+)$ is smaller than $B(\mathrm{E2}\ 2_1^+ \rightarrow 0_1^+)$. This discrepancy was already pointed out by Kalman *et al.* [20], who used the pairing interaction. Our

TABLE 2

Electromagnetic transition probabilities and static quadrupole moments of $^{20}$Ne

(a)

| $J_1$ \ $J_2$ | $2_1$ | $2_2$ | $2_3$ |
|---|---|---|---|
| $0_1$ | −9.12 | 0.098 | −0.657 |
| $0_2$ | 0.695 | −6.27 | 2.05 |
| $0_3$ | 0.964 | 0.409 | 1.89 |

(b)

| $J_1$ \ $J_2$ | $4_1$ | $4_2$ | $4_3$ |
|---|---|---|---|
| $2_1$ | −13.6 | 2.77 | −0.090 |
| $2_2$ | 0.428 | −3.83 | 6.31 |
| $2_3$ | 0.265 | 5.29 | 0.812 |

(c)

| $J_1$ \ $J_2$ | $6_1$ | $6_2$ | $6_3$ |
|---|---|---|---|
| $4_1$ | 14.9 | 1.39 | −0.37 |
| $4_2$ | 3.62 | −1.97 | −2.62 |
| $4_3$ | 0.90 | 9.91 | 1.78 |

(d)

| $J_1$ \ $J_1$ | $8_1$ | $8_2$ | $8_3$ |
|---|---|---|---|
| $6_1$ | −13.3 | 2.24 | −0.49 |
| $6_2$ | −1.00 | −10.0 | 2.80 |
| $6_3$ | 1.59 | 3.26 | 1.69 |

(e)

| $J_i \rightarrow J_f$ | $\Gamma_{\gamma\,\mathrm{obs}}(\mathrm{E2})$ | $\Gamma_{\gamma\,\mathrm{cal}}(\mathrm{E2})$ |
|---|---|---|
| $2_1 \rightarrow 0_1$ | 17.6 | 17.6 |
| $4_1 \rightarrow 2_1$ | 15.1 | 20.7 |
| $6_1 \rightarrow 4_1$ | 28±7 | 18.1 |
| $8_1 \rightarrow 6_1$ | | 11.0 |
| $0_2 \rightarrow 2_1$ | 3.8 | 0.51 |
| $2_2 \rightarrow 0_1$ | | 0.002 |
| $2_2 \rightarrow 0_2$ | | 8.32 |

(f)

| | $Q/e$ (b) | $Q_0/e$ (b) |
|---|---|---|
| $2_1$ | −0.16 | $0.55_2$ |
| $4_1$ | −0.20 | $0.55_0$ |
| $6_1$ | −0.22 | $0.54_4$ |
| $8_1$ | −0.22 | $0.52_2$ |

(g)

| $T_i$ | $J_i \rightarrow T_f$ | $J_f$ | $\Gamma_{\gamma\mathrm{exp}}(\mathrm{M1})$ | $\Gamma_{\gamma\mathrm{cal}}(\mathrm{M1})$ |
|---|---|---|---|---|
| 1 | $1_1 \rightarrow 0$ | $0_1$ | 0.36 | 0.23 |
| 1 | $1_2$ | | 0.015 | 0.012 |
| 1 | $1_3$ | | 0.0002 | 0.007 |
| 1 | $1_1 \rightarrow 0$ | $0_2$ | | 0.041 |
| 1 | $1_2$ | | | 0.026 |
| 1 | $1_3$ | | | 0.017 |
| 1 | $1_1 \rightarrow 0$ | $0_3$ | | 0.017 |
| 1 | $1_2$ | | | 0.0004 |
| 1 | $1_3$ | | | 0.006 |

(a), (b), (c) and (d) show calculated transition matrix elements $\langle J_i \| Q \| J_f \rangle$, where $Q$ is the quadrupole moment. Widths in (e) and (g) are measured in Weisskopf units. $Q_0$ are intrinsic quadrupole moments obtained from calculated $Q$ by a use of simple relation $\langle IM = I | Q | IM = I \rangle = -I/(2I+3)Q_0$.

calculation takes into account also the spin-orbit interaction, but this difficulty does not seem to be removed, and further study is required.

Recently an E2 transition from the 6.72 MeV first excited $0_2^+$ level to the 1.63 MeV $2_1^+$ level was observed [21]). This transition is strikingly enhanced (3.8 W.u.). The $SU_3$ model forbids this transition, but our wave functions are admixtures of different $(\lambda\mu)$ states. Therefore, we can find a non-vanishing E2 matrix between these states which is, however, only one seventh of the experimental value.

This case is very similar to the famous enhanced E2 transition in $^{18}$O from the first excited $0_2^+$ to the $2_1^+$ state, which was explained by an admixture of a core-excited state [14,15]). It is therefore an interesting problem to study the effect of the core-excited state in $^{20}$Ne, particularly the effect on the $B$(E2). This is being studied by one of the authors (A.A.) [22]).

Recently Hanna observed that the $T = 2,0^+$ state, which is an analogue state of $^{20}$O, can decay into a $T = 1$, $J^\pi = 1^+$ state, which further decays into the ground state by means of an M1 transition [23]). He found only one strong M1 transition to the ground state. Table 2(g) shows that among many possible M1 transitions which decay to the ground state, only one of them has considerable strength. This is very analogous to the well-known 15.1 MeV M1 transition to the ground state in $^{12}$C [ref. [24])]. This fact can be understood as follows. The most important term in the M1 operator is $\sum_i \tau_{3i}\sigma_i$, which cannot change the spacial symmetry or the $SU_4$ symmetry and the orbital wave function. Therefore, the main component [4] (80) $^{11}S_{J=0}$ in the ground state cannot be excited through this operator $\sum \tau_i\sigma_i$ into states with $T = 1$, $J = 1$, which cannot have the [4] symmetry, although this excitation can be induced by $\sum \tau_i l_i$, which is relatively less important. The M1 transition can occur thus through the admixed component of [31], which is admixed of course by the spin-orbit interaction. Table 4 shows that only the (61) $^{13}P_{J=0}$ state dominates among the [31] symmetric states in the ground state. This means that only one state with (61) $^{33}P_1$ can be reached by the M1 transition. Simple selection rules would lead one to believe that the M1 transition leads also to the (61) $^{31}P_1$, but it is very interesting to observe that this is not theoretically possible, in other words, the matrix element of $\sum \tau_i\sigma_i$ between the $^{31}P_{J=1}$ and $^{13}P_{J=0}$ states vanishes. This selection rule seems to be more general, i.e. the matrix element of $\sum \tau_i\sigma$ vanishes between $^{31}$P and $^{13}$P in the [4$^\kappa$31] symmetry. Although the $SU_3$ and the orbital symmetries are not very good in the $T = 2$ states, the main component in the lowest $T = 2$, $J = 0$ state is the [22], (42) $^{51}S_0$ state, which can decay into only the [22], (42) $^{33}S_1$ which is admixed in the [3, 1] $T = 1$, $S = 1$, $J = 1$ state. Among low-lying $T = 1$, $J = 1$ states, which have the [31] symmetry as the main component, there are a few states which contain this [22] (42) $^{33}S_1$ state. There is, however, no state containing [31] (61) $^{33}P_1$ as the main component and a considerable amount of [22] (42) $^{33}S_1$ except the lowest $T = 1$ $J = 1$ state, which has the largest M1 strength to the ground state. Therefore, there is only one strong cascade M1 transition from $T = 2, 0^+$ to the ground state. The important fact in this explanation is that the spin-orbit interaction can

connect only (61) of [31] with (80) of [4] in the ground state. We can expect that the cascade scheme must be more complicated in alpha magic nuclei in which the leading $SU_3$ $(\lambda\mu)$ state has non-vanishing $\mu$, because a few different $(\lambda'\mu')$ states in the next highest symmetry can be admixed. This means that for example in $^{24}$Mg, at least three different $(\lambda\mu)$ states in [431] must have considerable admixture in the ground state, and thus the M1 cascade can proceed a few $T = 1$, $J = 1$ states. This is confirmed by the experiment of Hanna.

## 5. Truncation

It is important and interesting to extend our shell-model calculations beyond $^{20}$Ne. The shell-model bases are, however, very large for nuclei heavier than $^{20}$Ne [ref. [25])]. Table 3 shows the dimensions of the energy matrices involved in the shell-model calculations of the six-particle system. Some of them are larger than 500. In $^{24}$Mg, for example, the matrices will often exceed $2000 \times 2000$. This is an explosion

TABLE 3
Number of the shell-model basis in six-particle systems

| $J$ | $T$ | | | |
|---|---|---|---|---|
| | 0 | 1 | 2 | 3 |
| 0 | 71 | 148 | 54 | 14 |
| 1 | 243 | 351 | 164 | 19 |
| 2 | 307 | 525 | 219 | 33 |
| 3 | 366 | 537 | 232 | 29 |
| 4 | 311 | 502 | 195 | 26 |
| 5 | 259 | 369 | 144 | 12 |
| 6 | 169 | 255 | 82 | 8 |
| 7 | 107 | 135 | 41 | 1 |
| 8 | 47 | 67 | 14 | |
| 9 | 24 | 21 | 3 | |
| 10 | 5 | 6 | | |
| 11 | 1 | | | |

problem of the shell-model states. It is not only technically difficult but also may be too lavish to treat all these states on an equal footing, because we can only compare calculated results with two or three experimental data. It is therefore most desirable to find a more physical way to avoid this explosion problem. Two concepts are studied again in $^{20}$Ne to search for a suitable truncation. These were already thoroughly studied in our first paper [2]). The first is based on the symmetric group or the super-multiplet theory introduced by Wigner [6]). The other is the classification according to the $SU_3$ group found by Elliott [7]). Wave functions of $^{20}$Ne with low energy are analysed in terms of the symmetry in table 4. The percentages of the highest symmetry [4] and the next-highest symmetry [31] are over 98 % even in the worst

case, which is the $8^+$ state. The contribution coming from the next symmetry [31] cannot be neglected, because the spin-orbit interaction breaks the super-multiplet symmetry and induces strong couplings between the states of the highest symmetry and those of the next-highest symmetry. Our analysis confirms that the symmetry provides very good truncation. Table 4 also shows that it is necessary to include only a few $(\lambda\mu)$ of the irreducible representations of the $SU_3$ group to carry over 95 %

TABLE 4

Percentage analysis of the wave functions of low-lying states in $^{20}$Ne in terms of the $SU_3$ irreducible representations

| | | $0_1$ | $0_2$ | $2_1$ | $2_2$ | $4_1$ | $6_1$ | $8_1$ |
|---|---|---|---|---|---|---|---|---|
| [4] | (80) | 0.895 | 0.042 | 0.906 | 0.025 | 0.848 | 0.875 | 0.806 |
| | (42) | 0.016 | 0.828 | 0.018 | 0.717 | 0.061 | 0.008 | |
| | (04) | 0.025 | 0.053 | 0.004 | 0.105 | 0.001 | | |
| | (20) | 0.000 | 0.004 | 0.000 | 0.002 | | | |
| [31] | (61) | 0.059 | 0.014 | 0.068 | 0.041 | 0.082 | 0.110 | 0.174 |
| | (42) | 0.000 | 0.000 | 0.000 | 0.019 | 0.002 | 0.001 | |
| | (23) | 0.002 | 0.043 | 0.001 | 0.063 | 0.001 | 0.000 | |
| | (31) | 0.001 | 0.009 | 0.001 | 0.014 | 0.002 | 0.000 | |
| | (12) | 0.000 | 0.002 | 0.000 | 0.002 | 0.000 | 0.000 | |
| | (20) | 0.000 | 0.000 | 0.000 | 0.000 | 0.000 | 0.000 | |
| [22] | | 0.001 | 0.004 | 0.001 | 0.011 | 0.002 | 0.005 | 0.020 |
| [211] | | 0.001 | 0.001 | 0.001 | 0.001 | 0.001 | 0.001 | |
| [1111] | | 0.000 | 0.000 | 0.000 | 0.000 | 0.000 | 0.000 | |

of probability. Altogether, it is very reasonable to take (i) the most favorable state given by the $SU_3$ in the highest symmetry; i.e. the state of the leading representation, (ii) a few more states, which can be connected by the two-body interaction directly with the most favorable state and (iii) a few other states in the next symmetries, which have a direct interaction through the spin-orbit interaction with the most favorable state.

Recently Harvey and one of the authors (Sebe) have found that $(\lambda\mu)$ having $\lambda+2\mu$ = max are most important, thus indicating which $(\lambda\mu)$ have to be chosen in the truncation. The admixture of these representations seems to have a physical interpretation in terms of vibrations. The states which are employed in our calculation are shown in table 5. According to Harvey and Sebe, a few more $(\lambda\mu)$ should be added, for example (25) in [42] and (25) and (06) in [411]. These states are being included in our next calculation. Some states in tables 5 are omitted when the matrices thus obtained exceed $60 \times 60$ in order to save computing times.

The percentage analysis of wave functions of $^{22}$Ne are given in table 6, which indicates that many $(\lambda\mu)$ included in table 5 have completely negligible contributions in the low-lying states. Among 59 basis of $2^+$, which are spanned by the $(\lambda\mu)$ included in table 4, only 28 states have appreciable contributions, and the total probabilities of 21 other states are less than 0.5 %. We shall have only to take into

TABLE 5

The shell-model states employed in the present calculation

| Number of particle | Truncated set of states | | | | | | | | |
|---|---|---|---|---|---|---|---|---|---|
| 5 | [41] | (81) | (62) | (24) | (43) | (51) | (32) | (40) | | |
| | [32] | (62) | (43) | (24) | (32) | | | | | |
| | [311] | (43) | (70) | (51) | (32) | (32) | | | | |
| | [211] | (24) | (51) | (32) | | | | | | |
| 6 | [42] | (82) | (63) | $(44)_1$ | $(44)_2$ | (06) | (71) | (52) | $(60)_1$ | $(60)_2$ |
| | [411] | (90) | (63) | (71) | $(52)_1$ | $(52)_2$ | | | | |
| | [33] | (63) | (52) | | | | | | | |
| | [321] | (44) | (71) | | | | | | | |
| 7 | [43] | (83) | (64) | (45) | $(53)_1$ | $(53)_2$ | (26) | | | |
| | [421] | (91) | (64) | $(72)_1$ | $(72)_2$ | | | | | |
| | [331] | (72) | | | | | | | | |
| 8 | [44] | (84) | (73) | (46) | (81) | (54) | $(62)_1$ | $(62)_2$ | (08) | |
| | [431] | (92) | (65) | $(73)_1$ | $(73)_2$ | (46) | $(81)_1$ | $(81)_2$ | $(54)_1$ | |
| | | $(54)_2$ | $(54)_3$ | (27) | | | | | | |

TABLE 6

Percentage analysis of the wave functions of low-lying states in $^{22}$Ne in terms of the $SU_3$ irreducible representations

| | | $0_1^+$ | $0_2^+$ | $2_1^+$ | $2_2^+$ | $4_1^+$ | $4_2^+$ | $6^+$ |
|---|---|---|---|---|---|---|---|---|
| [42] | (82) | 0.707 | 0.059 | 0.752 | 0.768 | 0.732 | 0.762 | 0.723 |
| | (63) | | | 0.000 | 0.003 | 0.005 | 0.054 | 0.004 |
| | (71) | | | 0.001 | 0.000 | 0.005 | 0.001 | 0.019 |
| | $(44)_1$ | 0.044 | 0.441 | 0.018 | 0.024 | 0.005 | 0.021 | 0.001 |
| | $(44)_2$ | 0.064 | 0.210 | 0.029 | 0.059 | 0.004 | 0.019 | 0.000 |
| | (52) | | | 0.000 | 0.018 | 0.000 | 0.024 | 0.001 |
| | $(60)_1$ | 0.030 | 0.016 | 0.033 | 0.001 | 0.028 | 0.001 | 0.021 |
| | $(60)_2$ | 0.001 | 0.007 | 0.000 | 0.000 | 0.000 | 0.000 | 0.002 |
| | (06) | 0.000 | 0.163 | 0.000 | 0.000 | 0.000 | 0.000 | 0.000 |
| [411] | (90) | 0.048 | 0.043 | 0.064 | 0.001 | 0.092 | 0.000 | 0.109 |
| | (63) | 0.041 | 0.012 | 0.034 | 0.073 | 0.022 | 0.055 | 0.019 |
| | (71) | 0.017 | 0.027 | 0.023 | 0.014 | 0.039 | 0.011 | 0.045 |
| | $(52)_1$ | 0.002 | 0.002 | 0.001 | 0.000 | 0.000 | 0.001 | 0.002 |
| | $(52)_2$ | 0.001 | 0.006 | 0.000 | 0.000 | 0.003 | 0.001 | 0.007 |
| [33] | (63) | 0.032 | 0.010 | 0.030 | 0.030 | 0.025 | 0.036 | 0.024 |
| | (52) | 0.000 | 0.000 | 0.000 | 0.000 | 0.000 | 0.001 | 0.000 |
| [321] | (71) | 0.011 | 0.004 | 0.015 | 0.011 | 0.019 | 0.012 | 0.023 |
| | (44) | 0.002 | 0.000 | 0.000 | 0.000 | 0.000 | 0.001 | 0.000 |

$\xi = 2.0$, $\varepsilon = 0.0$, Gaussian; $^{13}V = 70$, $^{31}V = 52$, $^{11}V = 0$, $^{33}V = -26$.

account those 28 states in the future calculations of $T = 1$, $J = 2^+$ states in $^{22}$Ne. These observations prove again that the group $SU_3$ provides a very good truncated basis to make the shell-model calculation feasible.

## 6. The level structure of $^{21}$Ne

The calculation shows a reasonable match with the observations for the levels of $\frac{3}{2}$, $\frac{5}{2}$, $\frac{7}{2}$ and $\frac{9}{2}$, which build a rotational $K = \frac{3}{2}$ band (fig. 7). The fit is good with both the Gaussian and Yukawa interactions. The obvious trouble is a $\frac{1}{2}^+$ too low state.

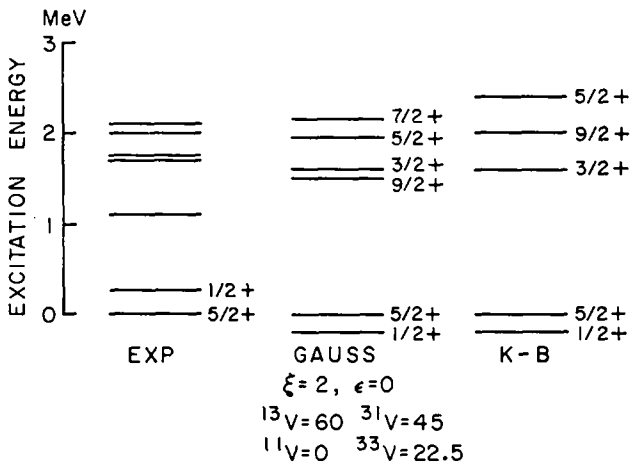


Fig. 6. Energy levels of $^{21}$F [ref. $^{31}$)].

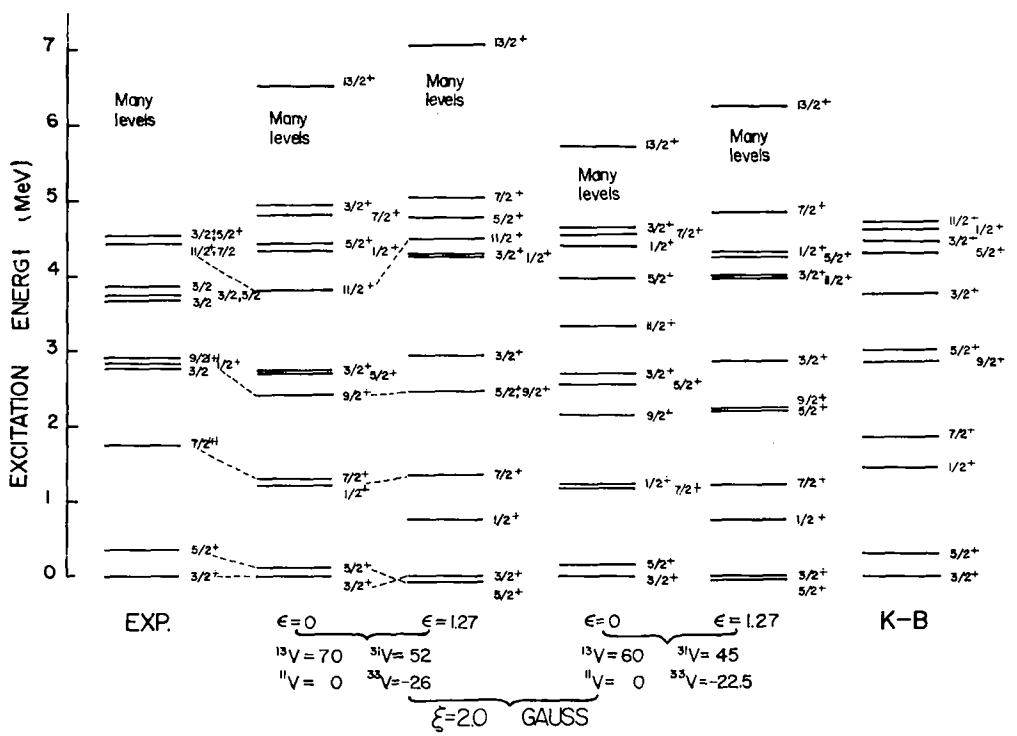


Fig. 7. Energy levels of $^{21}$Ne and $^{21}$Na [refs. $^{31,32,33}$)].

Because this level has a larger probability for finding an s-particle in it (consider simplest shell-model case), the energy of this level is very sensitive to the single particle energy of the s-orbit. The shift of this orbit to a higher energy relative to the d-orbit pushes up this level. The Gaussian interaction predicts a little better result than the Yukawa interaction.

An analogous situation was already found in $^{19}$O, where the $\frac{1}{2}^+$ level was too low.

It is very interesting to observe the same defect in the Oak Ridge result. The effective interactions derived by Kuo and Brown are, however, a little better than our phenomenological interaction to give a little higher energy to this $\frac{1}{2}^+$ level [8]). This suggests that their interactions produce the effect of pushing up the s-orbit, although not sufficiently.

## 7. The level structure of $^{22}$Ne and $^{22}$Na

The shell-model calculation fits the levels of $0^+$, $2^+$, $4^+$ and $6^+$. Although the Gaussian interaction gives better agreement with those states than the Yukawa interaction in fig. 8, the main reason for the differences is a different $\lambda$. The Yukawa interaction with a larger $\lambda$ gives almost the same result as the Gaussian interaction

TABLE 7

Percentage analysis of the wave functions of low-lying states in $^{22}$Na in terms of the $SU_3$ irreducible representations

| | | | $1_1$ | $1_2$ | $2_1$ | $3_1$ | $3_2$ |
|---|---|---|---|---|---|---|---|
| [42] | (82) | $J+1$ | 0.030 | 0.625 | 0.002 | 0.008 | 0.020 |
| | | $J$ | | | 0.765 | 0.006 | 0.086 |
| | | $J-1$ | 0.705 | 0.035 | | 0.741 | 0.677 |
| | (63) | $J+1$ | 0.007 | 0.126 | 0.021 | 0.001 | 0.006 |
| | | $J$ | 0.051 | 0.006 | 0.035 | 0.026 | 0.063 |
| | | $J-1$ | | | 0.030 | 0.066 | 0.014 |
| | (71) | | 0.007 | 0.008 | 0.000 | 0.006 | 0.001 |
| | $(44)_1$ | | 0.035 | 0.023 | 0.011 | 0.023 | 0.031 |
| | $(44)_2$ | | 0.059 | 0.056 | 0.044 | 0.027 | 0.018 |
| | (52) | | 0.000 | 0.000 | 0.000 | 0.004 | 0.013 |
| | $(60)_1$ | | 0.028 | 0.029 | 0.031 | 0.023 | 0.003 |
| | $(60)_2$ | | 0.001 | 0.001 | 0.001 | 0.000 | 0.000 |
| | (06) | | 0.000 | 0.000 | 0.000 | 0.000 | 0.000 |
| [411] | (90) | | 0.029 | 0.029 | | 0.027 | 0.006 |
| | (63) | | 0.015 | 0.020 | 0.027 | 0.012 | 0.032 |
| | (71) | | 0.001 | 0.002 | 0.002 | 0.000 | 0.000 |
| | $(52)_1$ | | 0.004 | 0.004 | 0.000 | 0.003 | 0.001 |
| | $(52)_2$ | | 0.002 | 0.001 | 0.000 | 0.001 | 0.000 |
| [33] | (63) | | 0.010 | 0.017 | 0.018 | 0.009 | 0.020 |
| | (52) | | 0.000 | 0.001 | 0.000 | 0.000 | 0.000 |
| [321] | (71) | | 0.014 | 0.013 | 0.010 | 0.016 | 0.006 |
| | (44) | | 0.001 | 0.004 | 0.003 | 0.001 | 0.002 |

$\xi = 2.0$, $\varepsilon = 0.0$, Gaussian; $^{13}V = 70$, $^{31}V = 52$, $^{11}V = 0$, $^{33}V = -26$.

for the $0^+$, $2^+$, $4^+$ and $6^+$ levels of the ground state rotational band. This $\lambda$ was defined in sect. 2.

A smaller $\varepsilon$ gives wave functions closer to the $SU_3$ values. The (82) $S$-component in the ground state is 60 % in intensity with $\varepsilon = 1.2$ and 71 % with $\varepsilon = 0.0$. The same is true in the other members of the ground state band (see table 7). A slightly stronger Gaussian interaction fits the rotational levels remarkably well as is shown in fig. 8 ($^{13}V = 70$, $^{31}V = 52$, $^{11}V = 0$, $^{33}V = -26$). Our calculation predicts another example of kinks. It is very desirable to observe the location of the $8^+$ state.

The moment of inertia in this gamma band which starts from $2^+$ seems to be given

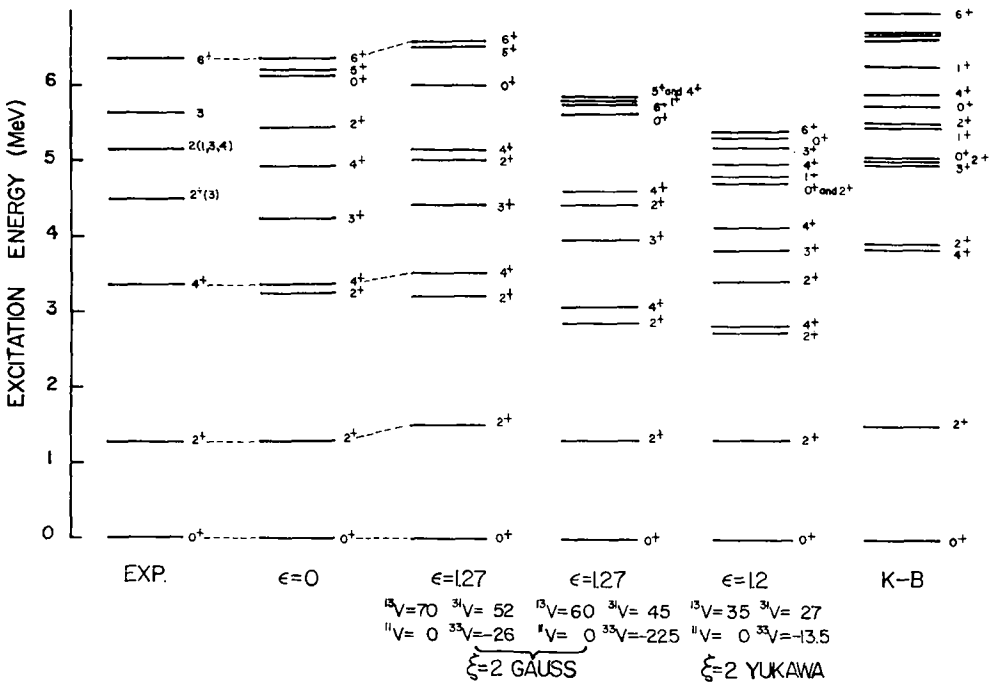


Fig. 8(a). Energy levels of $^{22}$Ne [refs. [31,33])].

reasonably well by the shell-model calculation (see fig. 8), but the whole band is predicted at too low an energy, which was expected by the extreme $SU_3$ model. The Oak Ridge Group encountered again the same kind difficulty and obtained the excited $K = 2$ band which is too low [8]).

Obvious trouble is found in the $T = 0$ levels for the doubly odd nucleus $^{22}$Na (fig. 9). The calculation predicts the two $1^+$ states lower than the state of $3^+$ which must be the ground state. According to the Nilsson model, the lowest expected sequence of spins is 3, 4, 5, 6 . . .. It is very interesting to observe that a reasonable fit is exhibited by the shell model for the sequence 3, 4 and $5^+$.

The lowest $T = 1$, $J = 0$ state, which is shown by the dotted line, is in the correct position relative to the $3^+$ state.

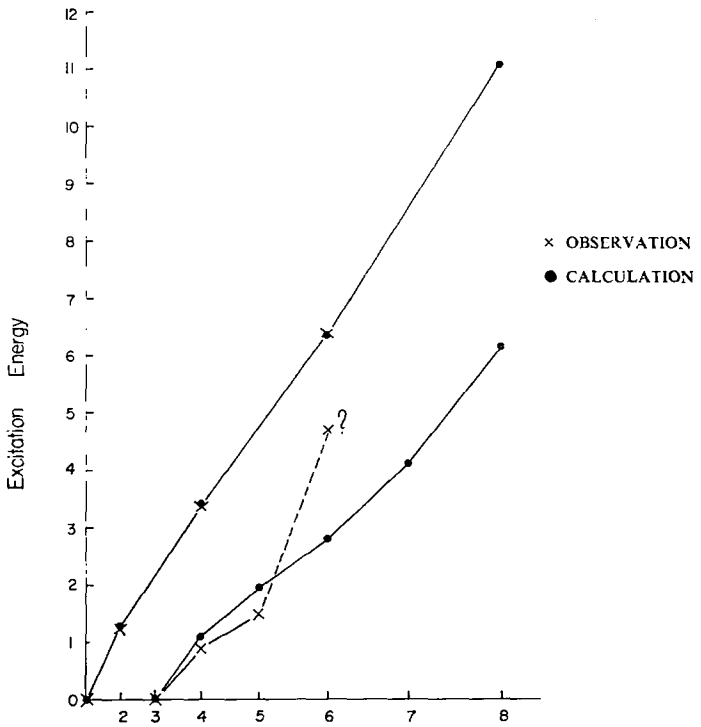


Fig. 8(b). Rotational levels of $^{22}$Ne and $^{22}$Na. The excited-state energies are plotted as a function of $I(I+1)$. In this figure $I$ is indicated instead of $I(I+1)$ in the abscissa.

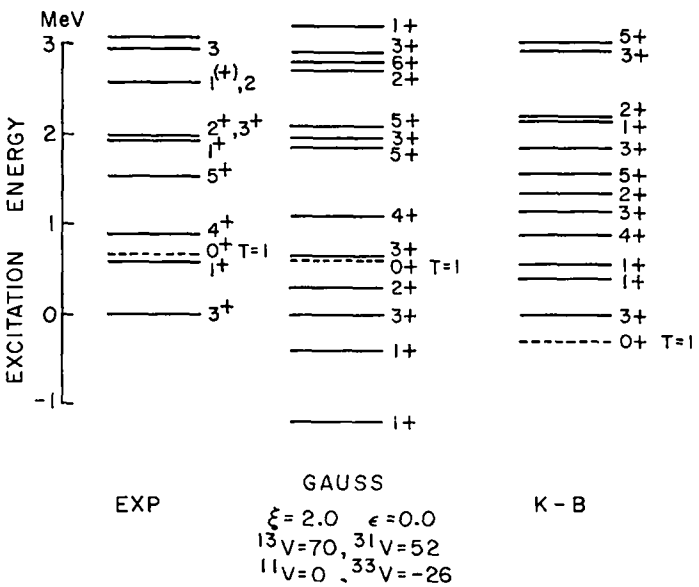


Fig. 9. Energy levels of $^{22}$Na [refs. [32,35])].

Again the Oak Ridge result shows the very similar situation in which the interaction derived by Kuo and Brown predicts two $1^+$ levels at almost the same energy, which is too low for one of them [8,9]). The lowest $T = 1$ state is not quite correct either.

The reason the shell model predicts two $1^+$ states too low is very easily understood. The $SU_3$ model provides the (82) $^{13}L_J$ states as the main ones in the low excitation energy. The attractive central interaction with short range favors, of course, lower L. Therefore, the $^{13}S_{J=1}$ state gains most of the interaction energy. Three levels $1^+$, $2^+$ and $3^+$ are expected to consist mainly of the (82) $^{13}D$ state. The spin-orbit interaction lowers the $3^+$ state most; the lowering of the $2^+$ state is next strongest. A detailed study of the wave functions shows, however, that the $1^+$ state of (82) $^{13}D_{J=1}$ is pushed down by the $1^+$ state of (63) $^{13}D_{J=1}$ through the central force and the spin-orbit interaction. If we increase the strength $\xi$ of the spin-orbit interaction ($\xi = 3.0$), the result is almost the same, and we fail to push up the $1^+$ state. It will be a future problem to explain the level structure of $^{22}$Na and in particular, how to push up the $1^+$ levels.

## 8. The level structure of $^{24}$Mg

Many published works study the structure of this nuclei [7,26,27]). Most of them are based on the $SU_3$ model. The level structure of $^{24}$Mg is of particular interest since the low-lying levels appear to be described well by the states belonging to the representation (84) of $SU_3$. This (84) representation produces three rotational bands; the first is the ground band with $K = 0$, the second the gamma band with $K = 2$, which explains qualitatively the observed structure, and the third the gamma band with $K = 4$.

Detailed calculations showed, however, that the second $2^+$ level is lying lower in energy than the lowest $4^+$ level, which is contrary to the experimental spin assignments.

TABLE 8

Interaction energies of the S-states of pure $SU_3$ states in $^{24}$Mg

| | | |
|---|---|---|
| [44] | (84) S | 68.36 MeV |
| | (46) S | 61.59 |
| | $(62)_1$S | 58.37 |
| | $(62)_2$S | 57.89 |
| | (08) S | 60.98 |

$\xi = 2.0$, $\varepsilon = 0.0$, Gaussian; $^{13}V = 70$, $^{31}V = 52$, $^{11}V = 0$, $^{33}V = -26$.

Wathne and Engeland [27]) carried out thoroughly the shell-model calculation taking into account all the possible states with the [44] symmetry. According to them, only the irreducible representations (84), (46), (08), (73) and (54) are important in the ground band and gamma band, although the excited $0^+$ states has a fairly large contribution from other $(\lambda\mu)$ states.

In the previous calculations [7,26,27]), the effect of the spin-orbit interaction was not taken into account. It is therefore very interesting to study how the spin-orbit interaction affects the level structure. We take then (84), (46), (08), (73), (54), (81) and $(62)^2$ in the [44] symmetry and (92), (65), $(73)^2$, $(81)^2$, $(54)^3$ and (27) in the [431] symmetry. Before the extensive calculation, it is worthwhile studying the kind of level structure predicted by taking only pure (84). The $0^+$, $2^+$, $4^+$ and $6^+$ states seem to build a rotational family, but the moment of inertia is too large. This situation is very familiar in the projected Hartree-Fock (HF) calculation [28,29]), which leads to

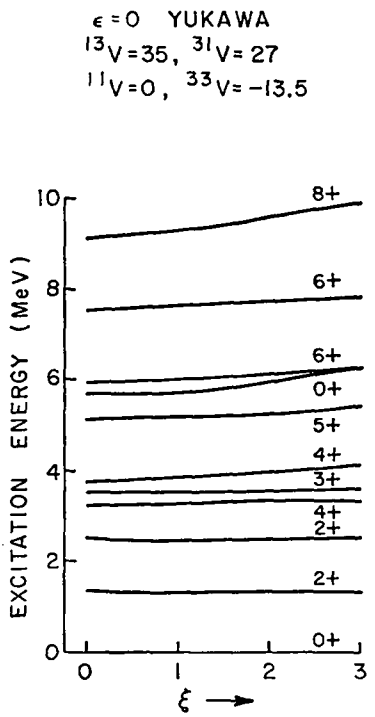


Fig. 10. Dependence of calculated energy levels of $^{24}$Mg on the spin-orbit interaction.

generally too large deformation and the level distances are, as a result, too small. In order to remove this difficulty, 2h-2p excitation, for example, should be taken into account. This similarity is very reasonable, because the wave functions given by the HF calculation are very close to the *LS* coupling limit. Ripka [28]) and Parik [29]) pointed out that there is a degeneracy in the HF solutions. One of the solutions is very similar to (84) and the other to (08). In the $SU_3$ calculation, we can find three low-lying $(\lambda\mu)$ states. Table 8 shows the calculated interaction energy of each band. Both (46) and (08) have very small excitation energies relative to (84). These excitation energies are, however, much larger than those predicted by the HF calculation.

Both the central force and the spin-orbit interaction induce mixing of different $(\lambda\mu)$ states. The mixing of these states tends to lower the ground state, which brings the first excited state to a reasonable position. Fig. 10 shows the dependence of the calculated level schemes on the strength $\xi$ of the spin-orbit interaction, where the Yukawa potential is used. It is clear from this figure that the calculated level schemes are very insensitive to this strength $\xi$.

On the other hand, calculated levels depend on $\varepsilon$ very much more than on $\xi$. This is shown in fig. 11, where the Yukawa potential is again assumed. There are two

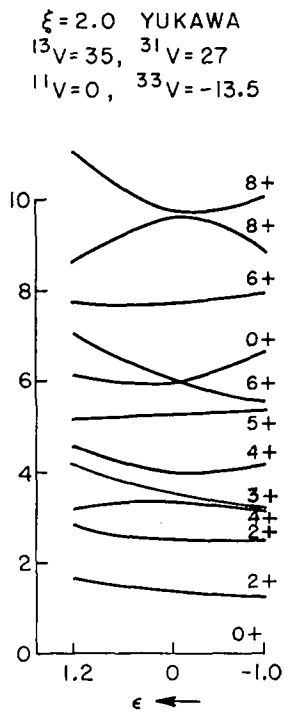


Fig. 11. Dependence of calculated energy levels of $^{24}$Mg on the single-particle level spacing between the s-orbit and the d-orbit.

ways one can choose a reasonable value for $\varepsilon$. The positions of higher angular momentum states $8^+$, $10^+$ and $12^+$ are particularly influenced by the quantity $\varepsilon$. Thus it is highly desirable in the first case to observe these higher angular momentum states experimentally. Furthermore, we note that when $\varepsilon$ is about zero, two $8^+$ states must be close to each other. A measurement of their separation would be a second way to fix $\varepsilon$.

The residual interaction with the Yukawa shape, which is fitted reasonably to two-, three- and four-body systems, gives poor agreement. Except the first excited state, the levels belonging to the lowest rotational band are predicted at too low energies. Disagreement is especially found in the case of $\varepsilon = 1.2$. Smaller $\varepsilon$ seems to

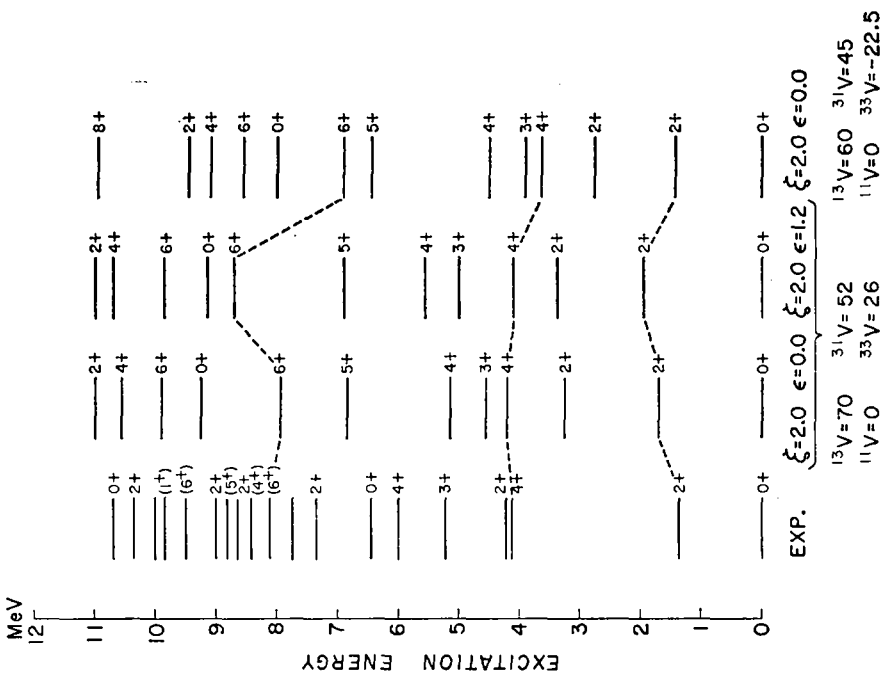


Fig. 13. Energy levels of $^{24}$Mg (for the Gaussian interaction).

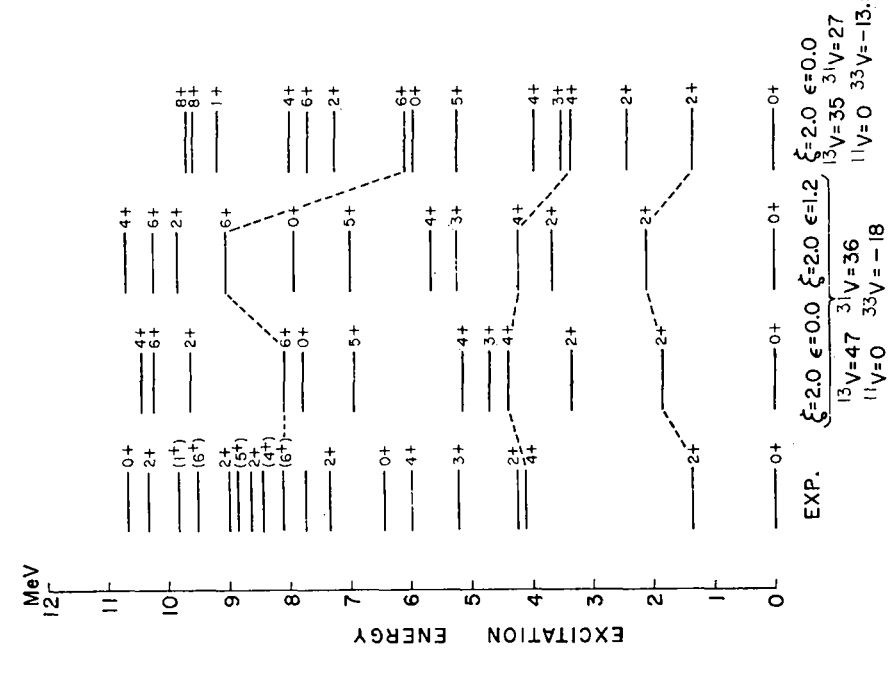


Fig. 12. Energy levels of $^{24}$Mg, [ref. [32])] (for the Yukawa interaction).

give better agreement with the observation. This situation has already been found in $^{21}$Ne and $^{22}$Ne.

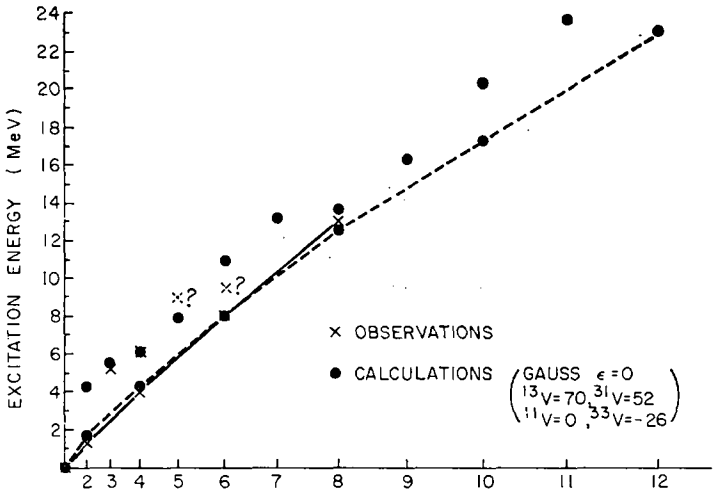


Fig. 14. Rotational level structure of $^{24}$Mg. The excited-state energies are plotted as a function of $I(I+1)$. In this figure $I$ is indicated instead of $I(I+1)$ in the abscissa.

TABLE 9
Variations of amplitudes of (84) in $^{24}$Mg as functions of $\varepsilon$

| State | | $\varepsilon$ 1.2 | 0 | −0.5 | −1.0 |
|---|---|---|---|---|---|
| $0^+$ | | 0.8037 | 0.8531 | 0.8678 | 0.8790 |
| $2^+$ | | −0.0065 | 0.0880 | 0.1111 | 0.1257 |
| | | 0.8404 | 0.8755 | 0.8822 | 0.8865 |
| $4^+$ | | 0.2268 | 0.0896 | 0.0110 | −0.0495 |
| | | 0.5275 | 0.3244 | 0.1919 | 0.0853 |
| | | 0.5731 | 0.8054 | 0.8685 | 0.8923 |
| $6^+$ | | −0.1028 | −0.1642 | −0.1716 | −0.1751 |
| | | 0.1708 | 0.0013 | −0.0362 | −0.0637 |
| | | 0.8564 | 0.8748 | 0.8757 | 0.8755 |
| $8^+$ | | 0.7399 | 0.7049 | 0.0772 | −0.0573 |
| | | 0.5937 | 0.5839 | 0.1001 | −0.1270 |
| | | 0.1295 | 0.2417 | 0.8978 | 0.8961 |
| $10^+$ | | −0.4449 | −0.3847 | −0.3790 | −0.3758 |
| | | 0.7513 | 0.7635 | 0.7560 | 0.7485 |
| $12^+$ | | 0.9479 | 0.9484 | 0.9486 | 0.9488 |

The comparisons between calculated and observed levels are given in fig. 12 for the Yukawa interaction and in fig. 13 for the Gaussian interaction. We know already that a slightly stronger interaction produces a better agreement in $^{22}$Ne. Therefore, we try to take a slightly stronger interaction. The results are exhibited in fig. 12 for Yukawa and fig. 13 for Gaussian interactions. In both cases, agreement becomes

much better, although the first excited state is a little higher than in the observation. The dependence on $\varepsilon$ is especially important for the $6^+$ state, and a comparison with the experiment suggests that $\varepsilon \approx 0$, where reasonable level structures are predicted by calculations. It is interesting to observe that the probability of (84) in the ground state is much larger (0.73) in $\varepsilon = 0$ than it is in $\varepsilon = 1.27$ (0.65) (table 9). Although the maximum angular momentum permissible in the eight-particle system is 12, the members of the ground state rotational band are observed only up to the $8^+$ state. As shown in fig. 14, the agreement is reasonable.

TABLE 10

Effect induced by the reduction of dimension on the excitation energies of $T = 0$, $J = 2^+$ states

| States \ Dimension | 30 | 53 |
|---|---|---|
| $2_1$ | 1.51 MeV | 1.37 MeV |
| $2_2$ | 2.69 | 2.52 |
| $2_3$ | 8.69 | 7.26 |
| $2_4$ | 10.51 | 9.32 |

The second $2_2^+$ level is still low. This difficulty is well known. It is, however, very interesting that all the $2^+$, $3^+$ and $4^+$ states of the gamma band are too low by nearly the same amount of energy. This recalls the analogous situation in $^{22}$Ne. In fig. 14, every state which is expected to belong to the $K = 2$ band is shifted upwards by 0.98 MeV. This shift produces beautiful agreement in the $3_1^+$ and $4_2^+$ states. It is an important unsolved problem to find a reason to push up these $K = 2$ bands both in $^{22}$Ne and $^{24}$Mg. It is extremely interesting to find kinks in this $K = 2$ band; $2^+, 4^+$, $6^+$ and $8^+$ seem to be shifted downward from locations of pure rotational states while $3^+$, $5^+$ and $7^+$ seem to be shifted upward.

Wathne and Engeland calculated branching ratios for E2 transitions and obtained reasonable agreement with observations except for the second $2^+$ state, for this latter state, the pure (84) gives very good agreement with observation, but when we mix other $(\lambda\mu)$ states, this agreement breaks down completely [27]). Our wave functions differ considerably from theirs. It is a very interesting problem for the future to calculate these branching ratios to test our wave functions.

We have taken a smaller number of basis states to study the changes induced in the energy spectrum. The states with $J = 2$ are taken as examples. Our truncation contains $53 \times 53$ matrices for $J = 2$ states. We reduce these matrices to those of dimension $30 \times 30$. Energy shifts are only about 100 keV both in the lowest $2^+$ and the next lowest $2^+$ states (table 10). This is because all the $(\lambda\mu)$ states which the spin-orbit interaction connects directly with the (84) state are already included among these 30 states, but some $(\lambda\mu)$ states which have direct interactions through the spin-orbit interactions with (73) and (46) are missing among the 30 states. This explains

very well why the lowest two states are very stable against this change of dimension, and other states are not. This confirms that as far as the lowest state is concerned, a dimension can be reduced to less than 30. This is very impressive when we consider the total number of states of $T = 0$ and $J = 2^+$ in the $(sd)^8$ configurations, which is 1206.

Furthermore, the percentage analysis of wave functions is shown in table 11, which confirms again that only a few $SU_3$ states are dominant. Particularly, it must

TABLE 11
Percentage analysis of the wave functions of low-lying states in $^{24}Mg$ in terms of the $SU_3$ irreducible representations

| | | $0_1$ | $0_2$ | $2_1$ | $2_2$ | $4_1$ | $4_2$ |
|---|---|---|---|---|---|---|---|
| [44] | (84) | 0.7278 | 0.1046 | 0.7743 | 0.7607 | 0.7619 | 0.7323 |
| | (46) | 0.1098 | 0.3793 | 0.0851 | 0.1002 | 0.1265 | 0.1380 |
| | (08) | 0.0475 | 0.3351 | 0.0225 | 0.0276 | 0.0037 | 0.0074 |
| | (73) | | | 0.0001 | 0.0036 | 0.0003 | 0.0196 |
| | (54) | | | 0.0000 | 0.0004 | 0.0000 | 0.0001 |
| | (81) | | | 0.0001 | 0.0000 | 0.0003 | 0.0003 |
| | $(62)_1$ | 0.0374 | 0.0709 | 0.0376 | 0.0241 | 0.0262 | 0.0221 |
| | $(62)_2$ | 0.0007 | 0.0100 | 0.0000 | 0.0011 | 0.0011 | 0.0023 |
| [431] | (65) | 0.0280 | 0.0037 | 0.0285 | 0.0323 | 0.0286 | 0.0311 |
| | (46) | | | 0.0003 | 0.0004 | 0.0039 | 0.0041 |
| | (27) | 0.0067 | 0.0564 | 0.0037 | 0.0048 | ** | ** |
| | (92) | 0.0178 | 0.0110 | 0.0205 | 0.0173 | 0.0213 | 0.0169 |
| | $(73)_1$ | 0.0199 | 0.0199 | 0.0225 | 0.0228 | 0.0220 | 0.0213 |
| | $(73)_2$ | 0.0031 | 0.0024 | 0.0035 | 0.0034 | 0.0035 | 0.0032 |
| | $(54)_1$ | 0.0002 | 0.0018 | 0.0001 | 0.0003 | 0.0002 | 0.0004 |
| | $(54)_2$ | 0.0008 | 0.0026 | 0.0009 | 0.0008 | 0.0000 | 0.0005 |
| | $(54)_3$ | 0.0001 | 0.0001 | 0.0000 | 0.0000 | 0.0002 | 0.0000 |
| | $(81)_1$ | 0.0002 | 0.0014 | 0.0003 | 0.0002 | 0.0002 | 0.0004 |
| | $(81)_2$ | 0.0000 | 0.0008 | 0.0000 | 0.0000 | 0.0001 | 0.0000 |

| | | $6_1$ | $6_2$ | 8 | 10 | 12 |
|---|---|---|---|---|---|---|
| [44] | (84) | 0.7923 | 0.8609 | 0.8960 | 0.7309 | 0.8996 |
| | (46) | 0.0692 | 0.0109 | 0.0005 | 0.0503 | |
| | (08) | 0.0027 | 0.0006 | 0.0000 | | |
| | (73) | 0.0165 | 0.0162 | 0.0013 | 0.1355 | |
| | (54) | 0.0005 | 0.0004 | 0.0003 | | |
| | (81) | 0.0018 | 0.0013 | 0.0101 | | |
| | $(62)_1$ | 0.0321 | 0.0134 | 0.0000 | | |
| | $(62)_2$ | 0.0011 | 0.0045 | 0.0057 | | |
| [431] | (65) | 0.0304 | 0.0211 | 0.0062 | 0.0367 | 0.0525 |
| | (46) | 0.0018 | 0.0003 | 0.0000 | 0.0021 | |
| | (27) | ** | ** | 0.0000 | 0.0008 | |
| | (92) | 0.0254 | 0.0295 | 0.0306 | 0.0278 | 0.0497 |
| | $(73)_1$ | 0.0213 | 0.0345 | 0.0420 | 0.0047 | |
| | $(73)_2$ | 0.0038 | 0.0055 | 0.0070 | 0.0038 | |
| | $(54)_1$ | 0.0001 | 0.0001 | 0.0000 | 0.0037 | |
| | $(54)_2$ | 0.0002 | 0.0002 | 0.0000 | 0.0000 | |
| | $(54)_3$ | 0.0000 | 0.0001 | 0.0000 | 0.0017 | |
| | $(81)_1$ | 0.0007 | 0.0003 | 0.0000 | 0.0018 | |
| | $(81)_2$ | 0.0001 | 0.0001 | 0.0003 | 0.0002 | |

$\xi = 2.0$, $\varepsilon = 0.0$, Yukawa; $^{13}V = 35$, $^{31}V = 27$, $^{11}V = 0$, $^{33}V = -13.5$.

be pointed out that these $(\lambda\mu)$ states with $\lambda+2\mu = 16$ carry over 85 % of the probabilities, and if we add (62) in [44] and (92), (73) in [431], they exhaust 98 % of the probabilities in these low-lying states.

## 9. Preliminary calculation of the level structure of $^{23}$Na

The level order is nicely reproduced for the first six levels; namely the ground state $(\frac{3}{2}^+)_1$, $(\frac{5}{2}^+)_1$, $(\frac{7}{2}^+)_1$, $(\frac{1}{2}^+)_1$, $(\frac{9}{2}^+)_1$ and $(\frac{3}{2}^+)_2$. During the calculation, an interaction is found to be strong between the (83) states and the (61) states, which are excluded in the present calculation. The results will be published separately elsewhere when these additional states will be taken into account.

## 10. Binding energy and residual interactions

Table 12 shows the observed binding energies relative to that of $^{16}$O after correcting the single-particle energy and the calculated values. The Yukawa interaction (6) gives reasonable agreement, while the Gaussian interaction (7) gives energies, which are a little too large. This is because the strength of the Yukawa interaction is adjusted to the binding energies of the two-body system, but no such attempt is made for the Gaussian interaction.

TABLE 12

Binding energies relative to that of $^{16}$O. The single-particle energies have been subtracted

| Nucleus | Exp (MeV) | Cal (MeV) | |
|---|---|---|---|
| | | Yukawa | Gauss |
| $^{18}$O | 7.97 | 8.11 | 8.81 |
| $^{18}$F | 8.92 | 9.05 | 10.26 |
| $^{19}$O | 9.81 | 9.68 | 10.55 |
| $^{19}$F | 17.25 | 18.40 | 21.43 |
| $^{20}$Ne | 31.38 | 33.25 | 39.34 |
| $^{21}$Ne | 36.03 | 36.98 | 43.76 |
| $^{22}$Ne | 44.29 | 45.16 | 53.05 |
| $^{22}$Na | 44.06 | 45.18 | 53.41 |
| $^{24}$Mg | 67.35 | 73.51 | 86.82 |

In nuclei heavier than the two-body systems of $^{18}$O and $^{18}$F, the binding energies already indicate that both Yukawa (6) and Gaussian (7) interactions are strong enough. Therefore, the residual interactions which give better results in the $^{22}$Ne and $^{24}$Mg level structures, introduce too much additional energy to give the correct binding energies.

Strengthening only the Q-Q interaction instead of all the parts of the interactions, however, we may obtain the same results concerning the level structure without increases in the binding energies.

We can expect three possible reasons to explain the introduction of this enhancement of the residual interaction in the middle of the shell. (i) Truncations. Beyond $^{20}$Ne, truncations are made to neglect many sd shell states. These truncations require

renormalization of the residual interaction. (ii) Higher-shell effect. Another possibility is due to excitations of sd shell particles into higher shells. It is interesting to study whether this mechanism produces large modifications in the effective interaction, particularly the Q-Q part of it and the three-body effect. (iii) Non-central interactions. As far as the central force and the spin-orbit interaction are concerned, we cannot expect that the additions of sd shell states which are neglected in the present calculation induce serious modification, because they have no direct couplings with the leading $SU_3$ states. The non-central interactions and the Majorana and Bertlett central interactions can have, however, direct couplings between the highest symmetric states (for example [44]) and lower symmetric states (for example [422]) which are completely neglected in this calculation. Effects induced by non-central interactions might be simulated by the renormalization of the central interactions.

It must be pointed out that the energy matrix elements of the singlet odd interaction $^{11}V$ is less than one tenth of the matrix elements of other interactions. As a result, this interaction cannot be determined.

Doubly even nuclei have either $[4^\kappa]$, $[4^\kappa 2]$ or $[4^\kappa 22]$ symmetry as the highest one. The total spin $S$ must be zero in those symmetries for the doubly even nuclei. Non-central interactions have no first-order effect, therefore, better agreement is found in the doubly even nuclei $^{20}$Ne, $^{22}$Ne and $^{24}$Mg. On the other hand, the highest symmetric states are $[4^\kappa 2]$ or $[4^\kappa 31]$ in doubly odd nuclei, where non-central interactions can have a noticeable effect even in the first order because the total spin $S$ can take non-vanishing values. The poor agreements in $^{20}$F and $^{22}$Na indicate the important roles of non-central interactions, even though they do not have serious effects in two- and three-body problems.

The effective interactions derived by Kuo and Brown give better agreements in general than simple phenomenological central interactions.

## 11. Discussion

The $(ls)$ interactions has non-vanishing matrix elements generally between certain $(\lambda\mu)$ and $(\lambda'\mu')$, where

$$(\lambda'\mu') = (\lambda+2\ \mu-1),\quad (\lambda+1\ \mu+1),\quad (\lambda+1\ \mu-2),$$
$$(\lambda-1\ \mu+2),\quad (\mu-1\ \mu-1),\quad (\lambda-2\ \mu+1).$$

All these matrix elements have the same order of magnitude, i.e. about 1 MeV.

The central interaction can connect $(\lambda\mu)$ with many other $(\lambda'\mu')$. It is found that the irreducible representations $(\lambda'\mu')$ with $\lambda'+2\mu' = \lambda+2\mu$ are important. Among them, the states with $\mu' = \mu+4$ and particularly $\mu' = \mu+2$ are admixed strongly by the central interaction. Non-diagonal matrix elements range from 1 MeV to 4 MeV.

At the same time, large matrix elements are found between $(\lambda\mu)$ and $(\lambda-2\ \mu-2)$, which reach 4 MeV. The pairing part of the interaction is responsible for this situation [30]).

The following prescription gives a reasonably good truncated basis: (i) the state of the leading representation $(\lambda\mu)$ of $SU_3$ in the highest symmetry, (ii) a few more states with $(\lambda'\mu')$ where $\lambda'+2\mu' = \lambda+2\mu$ in the highest symmetry, (iii) an additional state with $(\lambda-2, \mu-2)$ in the highest symmetry and (iv) a few other states with $(\lambda'\mu')$ in the highest if $S \neq 0$ and the next highest symmetries, where

$$(\lambda'\mu') = (\lambda+2\ \mu-1),\quad (\lambda+1\ \mu+1),\quad (\lambda+1\ \mu-2),$$
$$(\lambda-1\ \mu+2),\quad (\lambda-1\ \mu-1),\quad (\lambda-2\ \mu+1).$$

This prescription is good only in low $T$ states, for states with higher $T$ cannot have good spacial symmetries; an example of the latter is [22] in $^{20}$O. The result is that $2\lambda+\mu$ and $\lambda+2\mu$ cannot be large enough, and thus the state with $(\lambda\mu)$ is not especially favored.

Generally reasonable agreement with the observed level structures is obtained except for $0_2^+$ in $^{18}$O, $1_2^+$ in $^{18}$F, $(\frac{1}{2}^+)_1$ in $^{19}$O, $^{20}$F, $(\frac{1}{2}^+)_1$ in $^{21}$Ne, $2_2^+$ in $^{22}$Ne, $1_1^+$ and $1_2^+$, $^{22}$Na, $2_2^+$ and $3_1^+$ in $^{24}$Mg.

There must be degeneracy between two $2^+$ states belonging to the leading (82) representation in $^{22}$Ne and between three $2^+$ states of (84) in $^{24}$Mg in the pure Q-Q interaction. The central interaction and the spin-orbit interaction remove this degeneracy, but the induced energy separation between the $2_2^+$ state and $2_1^+$ state is still too small. This is a well-known difficulty of the $SU_3$ model. Full calculations without truncations, however, suffer from the same sort of trouble. Therefore, this difficulty does not seem to indicate an inadequacy of the $SU_3$ model but certain defects in the effective interaction or certain effects induced by higher excitations.

Another characteristic discrepancy concerns the $\frac{1}{2}^+$ states in $^{19}$O, $^{21}$Ne and $^{23}$Na. In all cases, the leading states should be $^{22}P_{\frac{1}{2}}$ ((41) for $^{19}$O, (81) for $^{21}$Ne and (83) for $^{23}$Na). The spin-orbit interaction $(ls)$ gives rather large energy differences between the $^{22}P_{\frac{1}{2}}$ and the $^{22}P_{\frac{3}{2}}$ states. These differences amount to $\xi$ in $^{19}$O, $0.9\xi$ in $^{21}$Ne and $\frac{1}{3}\xi$ in $^{23}$Na, respectively. Taking 2 MeV as the value of $\xi$, we obtain 2 MeV in $^{19}$O, 1.8 MeV in $^{21}$Ne and 0.67 MeV in $^{23}$Na, while the observed differences are 1.3 MeV, 2.8 MeV and 2.4 MeV, respectively. The $(ls)$ interaction seems to explain only partially these energy differences except $^{19}$O. Situations become more complicated after taking into account the $^{22}S_{\frac{1}{2}}$ state, which competes with the $^{22}P_{\frac{1}{2}}$ state, because the residual interaction favors the S-state. The interaction between the $^{22}P_{\frac{1}{2}}$ and $^{22}S_{\frac{1}{2}}$ states pushes down the $(\frac{1}{2})_1$ state. This contradicts the observations. It is still mysterious why $(\frac{1}{2})^+$ states have such high excitation energies.

We would like to thank Professor T. Inoue for his interest in this work. This series of calculations is being carried out with his continued cooperation. The authors are very much indebted to Dr. M. Harvey for stimulating discussions and a careful reading of our manuscript.

This work has been carried out under the support of the Nishina Memorial Fund and the Annual Research Project in 1965 and 1966 of the Institute for Nuclear Study.

The main calculations were performed by the use of HITAC 5020E in the University of Tokyo and additional calculations by IBM 360 67 at Princeton University.

One of the authors (A.A.) expresses sincere thanks to Professors P. Weiss and G. Temmer for their kind hospitality at Rutgers, The State University, under the support of the U.S. National Science Foundation. Thanks also to Professor G. Brown for his kind arrangement, which made it possible for us to use the computing center at Princeton University and for his stimulating discussions, and to Professor S. Yoshida for his continued encouragement and stimulating discussions.

One of the authors (T.S.) wishes to thank Drs. L. G. Elliott and H. H. Clayton for the hospitality extended to him at the Chalk River Nuclear Laboratories.

One of the authors (Y.A.) would like to express his hearty thanks to Professor T. Hecht for the visit at the University of Michigan.

Our thanks are due to Dr. E. Halbert and her colleagues for informing us of their very interesting results before publication and Dr. J. G. Pronko for providing the information about the $\frac{11}{2}^+$ state of $^{21}$Ne.

## References

1) J. P. Elliott and B. H. Flowers, Proc. Roy. Soc. **A229** (1955) 536;
M. G. Redlich, Phys. Rev. **99** (1955) 1427
2) T. Inoue, T. Sebe, H. Hagiwara and A. Arima, Nucl. Phys. **59** (1964) 1; **85** (1966) 184
3) I. Inoue, T. Sebe, K. K. Huang and A. Arima, Nucl. Phys. **A99** (1967) 305
4) S. Cohen, R. Lawson, M. Macfarlane and M. Soga, Phys. Lett. **9** (1964) 180
5) A. Arima, S. Cohen, R. Lawson and M. Macfarlane, Nucl. Phys. **A108** (1968) 94
6) E. P. Wigner, Phys. Rev. **51** (1937) 106
7) J. P. Elliott, Proc. Roy. Soc. **A245** (1958) 128, 562;
J. P. Elliott and M. Harvey, Proc. Roy. Soc. **A272** (1963) 557;
M. Harvey, Advances in nuclear physics, vol. 1. (Plenum Press, New York, 1968)
8) E. C. Halbert, Proc. Third Int. Sympos. on the structure of low medium mass nuclei, University of Kansas, Lawrence, Kansas (April 1968);
E. C. Halbert, J. B. McGrory and B. H. Wildenthal, Phys. Rev. Lett. **20** (1968) 1112
9) T. T. S. Kuo and G. E. Brown, Nucl. Phys. **85** (1966) 40
10) J. Nachamkin and M. Harvey, private communication
11) M. C. Bouten, J. P. Elliott and J. A. Pullen, Nucl. Phys. **A97** (1967) 113
12) Y. Akiyama, Nucl. Data **A2** (1966) 403
13) T. Hecht, Nucl. Phys. **62** (1965) 1
14) G. E. Brown, Proc. Paris Conf. on nuclear structure (1964) 129;
T. Engeland, Nucl. Phys. **72** (1965) 68
15) P. Federman and I. Talmi, Phys. Lett. **15** (1965) 165; **19** (1965) 490
16) L. Zamick, Phys. Lett. **19** (1965) 580
17) A. Arima, H. Horiuchi and T. Sebe, Phys. Lett. **24B** (1967) 129
18) A. Arima and I. Hamamoto, Nucl. Phys. **A112** (1968) 481
19) J. A. Kuehner and J. D. Pearson, Can. J. Phys. **42** (1964) 477
20) L. S. Kalman, J. P. Bernier and M. Harvey, Can. J. Phys. **45** (1967) 1297
21) T. K. Alexander *et al.*, Gatlinburg Conf. on nuclear physics (1966)
22) A. Arima, G. E. Brown and D. Strottman, private communication
23) S. S. Hanna, private communication;
S. J. Skorka *et al.*, Nucl. Data **A2** (1967) 347
24) M. Kawai and T. Terasawa, Prog. Theor. Phys. **22** (1959) 513;
D. Kurath, private communication

25) M. Harvey and T. Sebe, private communication
26) M. K. Bannerjee and C. Levinson, Phys. Rev. **130** (1963) 130
27) C. Wathne and T. Engeland, Nucl. Phys. **A94** (1967) 129
28) G. Ripka, Advances in nuclear physics, Vol. **1** (Plenum Press, New York, 1968)
29) J. C. Parik, Phys. Lett. **25B** (1967) 181
30) C. M. Vincent, Nucl. Phys. **A106** (1968) 35
31) Nuclear Data Sheets, ed. by K. Way *et al.* (National Academy of Science, National Research Council, Washington, D.C.)
32) P. M. Endt and C. van der Leun, Nucl. Phys. **A105** (1967) 1
33) J. G. Pronko, C. Rolfs and H. J. Maier, Nucl. Phys. **A94** (1967) 561
34) S. Bull, D. Pelte and B. Povh, Nucl. Phys. **91** (1967) 319
35) E. K. Warburton, A. R. Poletti and J. W. Olness, Phys. Rev. **168** (1968) 1232
36) R. Middleton, L. M. Polsky, C. H. Holbrow and K. Bethge, Phys. Rev. Lett. **21** (1968) 1398